J AM COLL CARDIOL
1983;1(4).1090–8

Electrocardiographic Effects of Myocardial Ischemia Induced by Atrial Pacing in Dogs With Coronary Stenosis

I. Repolarization Changes With Progressive Left Circumflex Coronary Artery Narrowing

DAVID M. MIRVIS, MD, ROWLYN L. GORDEY, BS

Memphis, Tennessee

The electrocardiographic effects of tachycardia in normal dogs and in dogs with progressive coronary stenosis were studied. In five animals, left atrial electrodes were surgically implanted and body surface isopotential patterns were recorded from 84 torso electrodes; pacing at rates of up to 250 beats/min increased recorded voltages registered during the ST segment but did not alter the spatial distribution of these potentials. In 10 dogs, an ameroid constrictor was also implanted about the left circumflex coronary artery. One week after surgery, pacing to rates of 250 beats/min had no effect on ST segment isopotential patterns. However, 2 and 3 weeks postoperatively, when significant coronary constriction was anticipated, pacing-induced ST segment depression was recorded along the inferior anterior and posterior chest surfaces. Abnormal negative voltages were more intense at 3 than at 2 weeks, but the distribution of these abnormalities was unchanged. This pattern was consistent with the location of ischemic myocardium. Calculation of early (10 to 40 ms) ST segment slopes demonstrated that downsloping forms were recorded over most of the area with abnormal ST segment voltages, but that horizontal or upsloping depression occurred at the margins of the abnormal zones. The findings suggest that this canine model may be a useful analog to clinical exercise stress testing to aid in evaluating the significance of clinical electrocardiographic patterns.

An increasing heart rate in the presence of coronary artery stenosis is known to cause myocardial ischemia. Numerous carefully controlled experimental studies have defined the hemodynamic derangements leading to and the metabolic abnormalities resulting from this ischemia (1–9). In contrast, the electrocardiographic correlates of tachycardia-induced ischemia have not been as rigorously determined. These changes are of critical clinical importance, as they form a basis for detection of coronary artery disease by exercise stress testing. Therefore, we explored the body surface electrocardiographic effects of tachycardia induced by atrial pacing in dogs with and without coronary artery stenosis produced by ameroid constrictor devices (10–16). In this report we focus on the effects of these interventions on ventricular repolarization forces to define the electrocardiographic results and thereby to determine the values and limitations of this experimental model.

From the Section of Medical Physics, Division of Cardiovascular Diseases, Department of Medicine, University of Tennessee Center for the Health Sciences, Memphis, Tennessee. This work was supported by Research Grant HL20597 and Research Career Development Award HL00560 from the National Heart, Lung, and Blood Institute, National Institutes of Health, Bethesda, Maryland, and by a grant from the Tennessee Affiliate of the American Heart Association, Nashville, Tennessee. Manuscript received August 20, 1982; revised manuscript received October 26, 1982, accepted October 29, 1982.

Address for reprints: David M. Mirvis, MD, 956 Court Avenue, Room 2F18, Memphis, Tennessee 38163.

Methods

Fifteen adult dogs, weighing 16 to 20 kg, were studied. All were in good general health and free of parasites.

Surgical protocol. Anesthesia was induced by intravenous sodium pentothal (20 mg/kg body weight) and maintained by inhalation of a mixture of halothane, nitrous oxide and oxygen. We then performed a thoracotomy in the fourth left intercostal space and opened the pericardium. In all dogs, a custom-designed quadripolar pacemaker electrode was sutured to the left atrial appendage. Electrodes at opposite corners of the electrode plaque were connected electrically, resulting in effective cardiac pacing with generation of only small pacemaker artifacts on surface electrocardiograms; larger artifacts resulted in significant voltage offsets in the electrocardiographic recordings.

0735-1097/83/0401090-9$03 00

J AM COLL CARDIOL
1983;1(4):1090–8

In 10 dogs, we gently isolated the origin of the left circumflex coronary artery. An ameroid constrictor (10–16) with an internal diameter of 2.77 mm was placed about this vessel, approximately 10 mm from its origin. Direct observation and monitoring of a single lead surface electrocardiogram assured adequate flow through the vessel immediately after constrictor placement.

The pericardium and chest were routinely closed. Pacemaker electrode wires were tunneled subcutaneously from the incision site to the posterior neck, and were exteriorized and covered with a sterile dressing. All animals survived surgery and were ambulatory within 48 hours. None developed significant fever or infection at either the incision or the exteriorization site.

Electrocardiographic recordings. Before each recording session, we sedated the dogs with 1 to 2 cc of Innovar (20 mg fentanyl and 0.4 mg droperidol per cc); the dogs were then intubated and respired with 100% oxygen. Eighty-four silver-silver chloride electrodes were then fixed to the animal's shaven torso in 14 strips, each containing six electrodes. These strips extended from the level of clavicles to below the inferior rib margins. Additional electrodes were placed on the limbs to record standard limb leads and derive the Wilson central terminal potential. Positions of electrode strips were marked with permanent ink to permit serial reproducible recordings. The dogs were then placed in a suspension sling (Alice King Chatham, Inc.) to allow stable upright posture during recordings.

Fourteen seconds of electrocardiographic potentials were recorded. Signals were amplified by a bank of 87 low noise, differential (electrode versus Wilson central terminal potential) amplifiers (17). Gains were set at 1,000 to 16,000 under computer control so that the output filled the input range of the analog to digital converter. The analog data were converted to digital form at a rate of 500 samples/channel per second.

Experimental protocol. Electrocardiographic data were recorded before surgery and 7, 14 and 21 days after ameroid constrictor or atrial pacemaker placement. During sessions after surgery, atrial pacing was initiated at a rate slightly higher than spontaneous heart rate (usually 90 beats/min) with impulses 2.5 ms in duration and at an amplitude 25% above threshold. Rate was then increased in increments of 20 beats/min at 3 minute intervals to a maximal heart rate of 250 beats/min. If atrioventricular block occurred, atropine (0.5 to 2.0 mg) was administered intravenously and pacing continued. Electrocardiographic data were recorded during the last 14 seconds of pacing at each heart rate. Additional recordings were registered 4, 10 and 20 minutes after cessation of pacing.

Data analysis. Electrocardiographic waveforms in each lead with similar morphologic features as determined by an autocorrelation method (18) were averaged to reduce random noise. Onsets and offsets of PR, QRS and ST-T intervals were manually determined from plots of root-mean-square potential, and potentials during the terminal 20 ms period of the PR segment were averaged and used as a zero potential baseline (19). Linear baseline drift was corrected as described by Spach et al. (19).

Isopotential distributions were constructed at 2 ms intervals during the ST-T interval using a combined linear-bilinear interpolation routine (20). Isopotential contour lines were drawn at 0 and at + and − 10, 20, 40, 60, 100, 200, 400 and 600 microvolt (μV) levels.

Results

Control Group

Atrial pacing to rates of 230 to 250 beats/min was successfully achieved in all dogs without atrioventricular or intraventricular block. Rest QRS durations were unchanged during the 3 week postoperative experimental period.

Left precordial electrocardiogram. Electrocardiograms recorded from one left precordial electrode are presented in Figure 1. The selected baselines are identified by the dashed lines and the positions of the pacemaker artifacts are marked by arrows. The increasing heart rate (from 76 beats/min to 230 beats/min) had little effect on the QRST configuration; the ST segments remained elevated and upsloping. At high rates (lower panel), the pacemaker artifact and hence the following P wave became superimposed on the preceding ST segment or T wave, or both; only portions of the ST segment recorded before the artifact were used for later analysis.

Isopotential distributions (84 torso electrodes). Isopotential distributions, constructed from potentials sensed 40 ms into the ST segment during atrial pacing 14 days after surgery, are displayed in Figure 2. Plus and minus signs identify the positions of the 84 torso electrodes, with the sign corresponding to the polarity of the sensed potential. The center of each map is along the sternum as identified

Figure 1. Electrocardiographic signal recorded 14 days after surgery from a left precordial electrode on a control dog. Tracings were recorded before atrial pacing (**top**, heart rate = 76 beats/min) and during atrial pacing at rates of 170 and 230 beats/min (M). The selected baseline levels are identified by the **dashed lines**, and the positions of the pacemaker artifact are marked by **arrows**. ST segments remain upsloping at high rates.

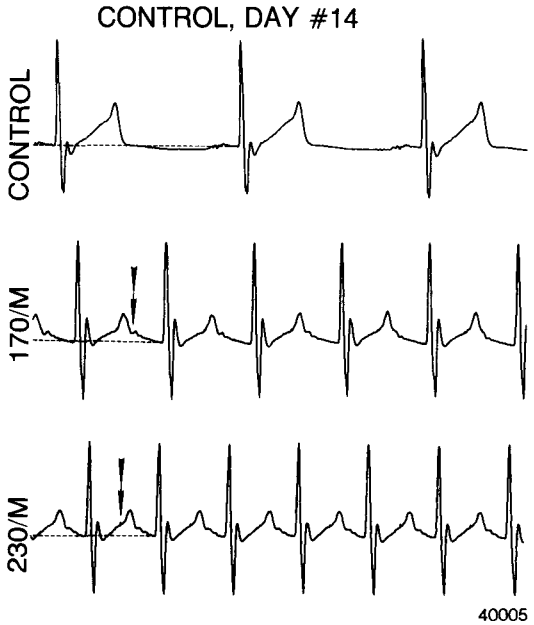

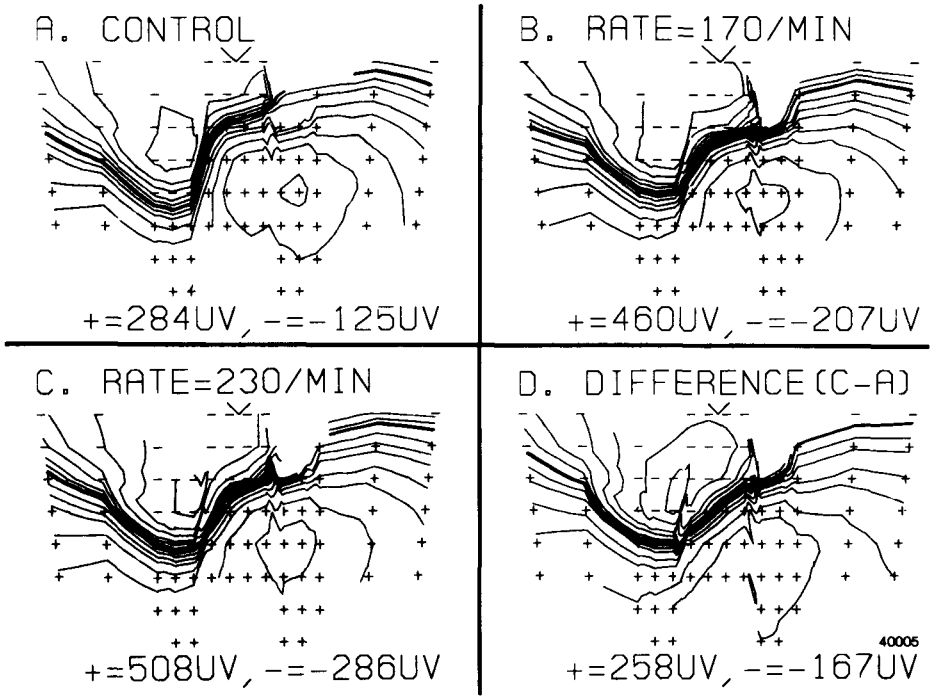

Figure 2. Isopotential distributions constructed from voltages recorded 40 ms into the ST segment from one control dog, 14 days after surgery. Markings and conventions are as described in the text. **Panel A**, Pattern at rest (heart rate 76 beats/min). **Panel B**, Distribution during atrial pacing at a rate of 170 beats/min. **Panel C**, Pattern at rate of 230 beats/min. **Panel D**, Isopotential "difference" map constructed by subtracting voltages of **A** from those of **C**.

by the "V," and the right and left edges of the map correspond to the left and the right paravertebral regions, respectively. Electrode strips were displaced inferiorly in axillary zones. Points at equal potential relative to the selected baseline are connected by solid contour or isopotential lines; the zero isopotential lines are overdrawn for emphasis. Magnitudes of peak positive and peak negative voltages are listed in each panel.

The distribution during spontaneous sinus rhythm at a rate of 76 beats/min is shown in Figure 2A. The left and inferior right hemithorax were covered by positive potentials and a single anterior maximal potential was located over the left precordium with a peak strength of 284 μV. Negative potentials overlie the right upper hemithorax; the single minimal potential had a strength of -125 μV. This bipolar or "dipolar" pattern was seen in all dogs at all postoperative dates.

Patterns in Figure 2B and C depict distributions 40 ms into the ST segment at paced rates of 170 and 230 beats/min. The pattern described previously was preserved with virtual constancy of the major map features' positions. However, both the maximum and minimum increased in strength as the rate was increased. Thus, peak positive voltage increased from 284 μV at rest (Fig. 2A) to 460 μV at 170 beats/min (Fig. 2B) and to 508 μV at 230 beats/min (Fig. 2C). Similiarly, negative potentials increased in absolute magnitude from -125 to -286 μV over this pacing range.

Isopotential difference map. To highlight the effects of rate on these repolarization patterns, voltages sensed by each electrode at rest (Fig. 2A) were subtracted from those of corresponding electrodes at peak heart rate (Fig. 2C). The resulting isopotential "difference" map, displayed in Figure 2D, depicts the effects of increasing rate. This pattern was characterized by a left anterior maximum (258 μV) and a right superior minimum (-167 μV). The positions of the extrema and the zero isocontour line closely corresponded to those at rest. Thus, tachycardia increased previously positive voltages and decreased (increased negativity) previously negative voltages. This pattern was consistent in all cases.

Slope of ST segment at each torso point. An additional spatial descriptor is depicted in Figure 3. Patterns in Figures 3A and B are isopotential distributions 10 and 40 ms into the ST segment at rest, respectively. The features are as previously described in Figure 2. Peak positive potential increased from 168 μV at 10 ms to 284 μV at 40 ms, while peak negative voltage increased from -161 to -125 μV. Patterns from Figure 3A were subtracted from Figure 3B, and the resultant distribution is displayed in Figure 3C. This distribution corresponds to the change in voltages at each point during the 30 ms interval between Figures 3A and B, depicting the slope of the ST segment at each torso point. Positive voltages in Figure 3C thus identify sites with upsloping ST segments, and negative potentials identify loci with downsloping segments.

Figure 3C demonstrates that the ST segment was normally upsloping at all but the most superior torso zones. Peak positive slope occurred along the left sternal border and equaled 115 μV/30 ms, or 3.83 mV/s. This pattern persisted at increased rates in all cases.

J AM COLL CARDIOL
1983,1(4):1090–8

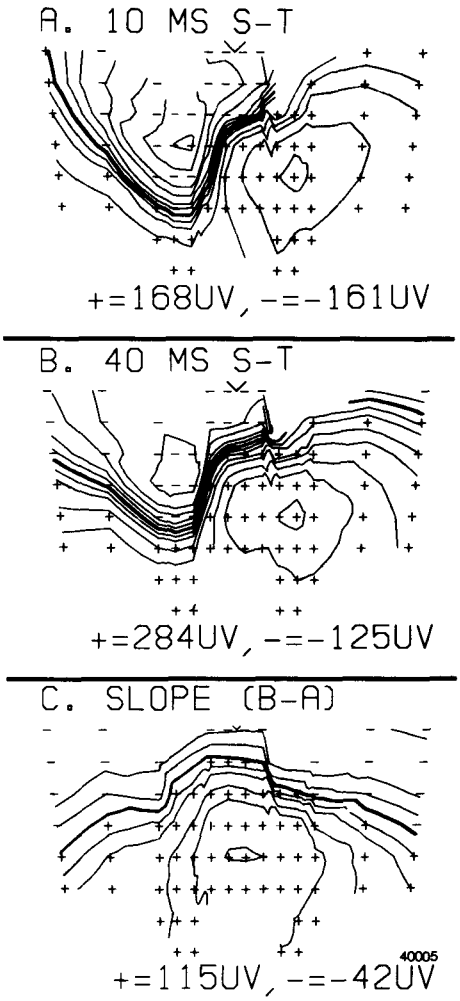

Figure 3. Panel A, Isopotential distribution at rest, 10 ms into the ST segment. **Panel B**, Isopotential pattern 40 ms into the ST segment. **Panel C**, Distribution constructed by subtracting voltages of **Panel A** from those of **B**, corresponding to the slope of the intervening ST segment. Markings are as in Figure 2 and as described in the text.

Ameroid Constrictor Group

All 10 dogs in which a left circumflex artery constrictor was placed survived surgery and appeared well 1 week later. Two died suddenly during the third week; the others remained overtly healthy. Atrial pacing to rates of over 210 beats/min was achieved in all eight surviving dogs at 1, 2 and 3 weeks postoperatively. None developed spontaneous or pacing-induced intraventricular conduction defects.

Single lead recordings. Single lead recordings from a left precordial electrode before and during atrial pacing, 21 days after ameroid constrictor placement, are presented in Figure 4. At rest (rate = 110 beats/min), the ST segment was slightly elevated above the baseline (dashed line), a normal finding at that locus. Atrial pacing at 170 beats/min resulted in no change. However, at a rate of 230 beats/min, significant downsloping ST segment depression occurred without alterations in the QRS configuation. Within 4 minutes after pacing was stopped, ST segment configuration normalized. However, T wave patterns remained different from control in this record; such differences uniformly reverted within 10 to 20 minutes after pacing ended.

Isopotential distributions 1 week after coronary constriction. Isopotential distributions constructed from voltages recorded 40 ms into the ST segment 1 week after ameroid placement are depicted in Figure 5. At rest (Fig. 5A), the distribution was as described in Figure 2A; positive potentials dominate the anterior chest, with negative voltages being registered over the upper back. Pacing at a rate of 190 beats/min (Fig. 5B) and at a rate of 250 beats/min (Fig. 5C) did not alter this pattern; positions of extrema remained stable. However, strengths of maxima and minima did increase progressively from 204 to 535 μV and from -102 to -126 μV. This was also noted in control dogs. Thus, 1 week after constrictor placement, the response to rapid atrial pacing was identical to that observed in the control group dogs.

Isopotential distributions 2 weeks after coronary constriction. Two weeks after surgery, however, atrial pacing did produce significant electrocardiographic abnormalities. Isopotential maps, again depicting voltages sensed 40 ms into the ST segment, are displayed in Figure 6. Patterns at rest (Fig. 6A) were unchanged from those 1 week after

Figure 4. Electrocardiographic recordings from a left precordial electrode 21 days after implantation of an ameroid constrictor on the left circumflex coronary artery (LCX). Tracings are 1) before atrial pacing (CONTROL), 2) during pacing at 170 beats/min, 3) during pacing at 230 beats/min, and 4) 4 minutes after cessation of pacing (RECOV.). **Dashed lines** identify the baseline level and **arrows** point to pacemaker artifacts.

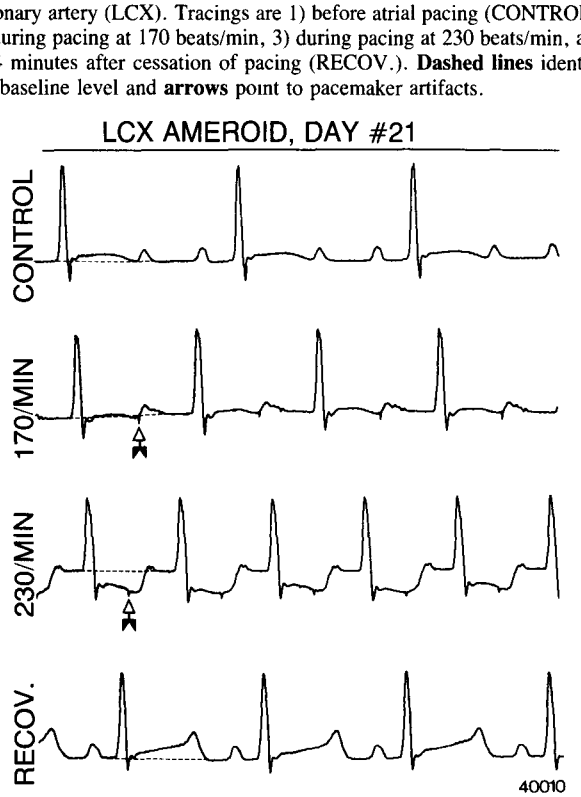

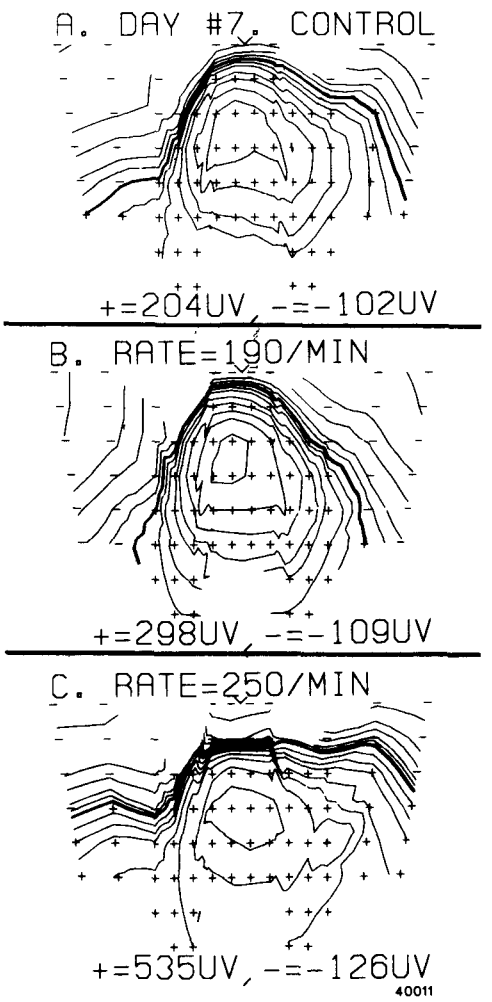

Figure 5. Body surface isopotential maps depicting potentials sensed 40 ms into the ST segment 1 week after implantation of an ameroid constrictor on the left circumflex coronary artery. **Panel A**, At rest (heart rate 70 beats/min). **Panels B and C**, During atrial pacing at rates of 190 and 250 beats/min, respectively.

surgery. Similarly, the distribution recorded at a paced rate of 190 beats/min (Fig. 6B) was unchanged from that described in Figure 5B. At rates of 210 beats/min and above, the patterns differed. The map in Figure 6C was recorded at a paced rate of 250 beats/min. Positive potentials were recorded on the upper anterior and posterior torso, and negative voltages were sensed along the entire inferior chest. The abnormal negative potentials increased progressively as rate increased, having peak values of -55, -64 and -137 μV at rates of 210, 230 and 250 beats/min, respectively. Thus, 2 weeks after ameroid constrictor placement, rapid atrial pacing did produce electrocardiographic evidence of myocardial ischemia not found earlier after surgery or in control dogs. Magnitudes of these abnormal potentials varied from -68 to -248 μV at the peak paced rate in the 10 experimental animals. The map in Figure 6D was recorded 4 minutes after cessation of pacing. Return of the pattern features to those recorded before pacing (Fig. 6A) was virtually complete.

Isopotential distributions 3 weeks after coronary constriction. The response to atrial pacing 3 weeks after surgery is shown in Figure 7. Patterns at rest (Fig. 7A) differed little from those previously described, although the maximum was more intense than at 2 weeks (334 versus 216 μV). Pacing at a rate of 210 beats/min or higher resulted in changes similar to those described in Figure 6, but the magnitudes of the abnormal voltages were greater. Thus, at a rate of 250 beats/min (Fig. 7B), negative voltages dominated the entire inferior half of the torso. Peak negative voltages now measured -368 μV. In the 10 animals, the maximal negative voltages at the highest paced rate varied from -101 to -381 μV and were significantly greater ($p < 0.01$) than those 1 week earlier.

Isopotential difference maps emphasizing these effects of pacing are presented in Figure 8. In Figure 8A, the differences between potentials at rest 2 weeks after surgery (Fig. 6A) and those at a paced rate of 250 beats/min (Fig. 6C) are displayed. Pacing generated an electrical field characterized by inferior negativity with peak voltages located on the left anterolateral torso. Magnitudes of the minimum at peak rate varied from -109 to -346 μV. The patterns in Figure 8B and C were computed by subtracting the pattern at rest 3 weeks after surgery (Fig. 7A) from those sensed at rates of 230 and 250 beats/min, respectively. The pattern is the same as that recorded 1 week earlier. However, the intensity of the abnormal minimum increased with increasing rate; for example, -214 μV at 230 beats/min and -613 μV at 250 beats/min.

Slope of ST segment at each torso region. The "isoslope" map (constructed as described for Fig. 3) displayed in Figure 9A was computed from potentials sensed during atrial pacing at a rate of 250 beats/min, 3 weeks after constrictor placement. ST segments recorded from electrodes over the midanterior chest and lower right and left back were characterized by a negative slope. Those from sites over the upper torso regions had upsloping characteristics. Peak negative slope equaled -66 μV/30 ms, or -2.2 mV/s. In Figure 9B, the isopotential distribution 40 ms into the ST segment during the same pacing episode as in Figure 9A is displayed. This is the same map as in Figure 7B. The shaded area identified zones in which 1) ST segment depression occurred (negative voltages on the isopotential map), and 2) the ST segment was upsloping (positive potentials on the isoslope map [Fig. 9A]). Thus, the ST segment was downsloping in most areas in which abnormal negative voltages were recorded, whereas zones on the border of the abnormal minimal had upsloping or horizontal ST segment configurations.

The percent of torso surface with this discordant pattern between ST segment voltage and slope equaled 16.7 $\pm$ 7.1% (mean $\pm$ 1 standard deviation; range = 8.2 to 31.4)

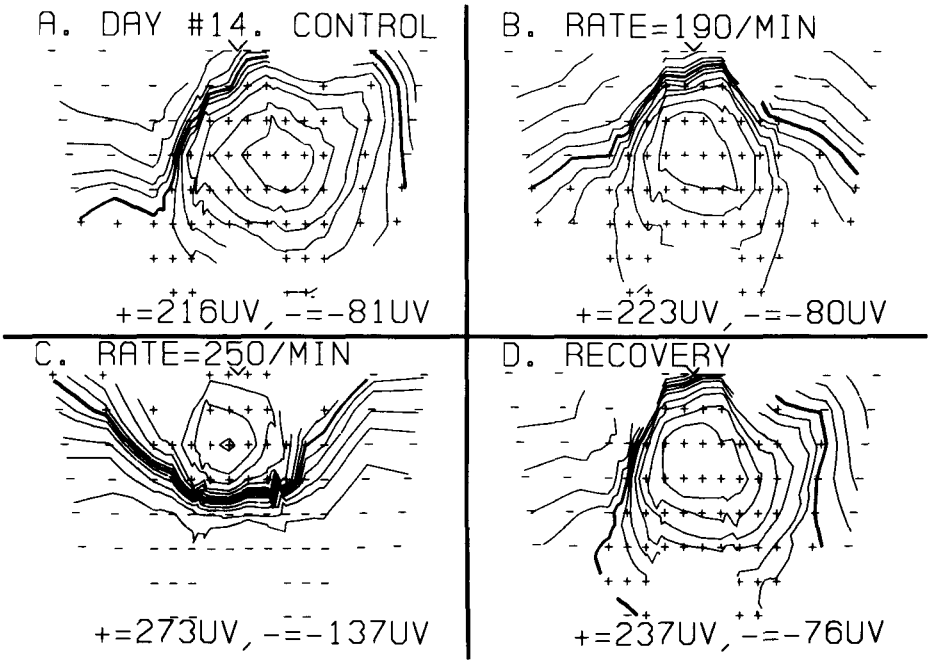

Figure 6. Isopotential patterns 40 ms into the ST segment 2 weeks after ameroid placement. **Panel A**, At rest (heart rate 94 beats/min). **Panels B and C**, During atrial pacing at rates of 190 and 250 beats/min, respectively. **Panel D**, 4 minutes after termination of pacing (heart rate 96 beats/min).

2 weeks after surgery at peak paced rate. In more superior torso zones, ST segments were elevated with negative slopes. This second discordant pattern was observed in 24.1 ± 6.8% of the torso surface.

Animals were sacrificed after the 3 week study period. The left circumflex artery was occluded or markedly narrowed at the site of ameroid constriction in all cases. Patterns in dogs with complete and with subtotal obstruction did not differ.

Figure 7. Isopotential distributions 40 ms into the ST segment 3 weeks after ameroid constrictor implantation. **Panel A**, At rest (heart rate 110 beats/min). **Panel B**, During atrial pacing at a rate of 250 beats/min.

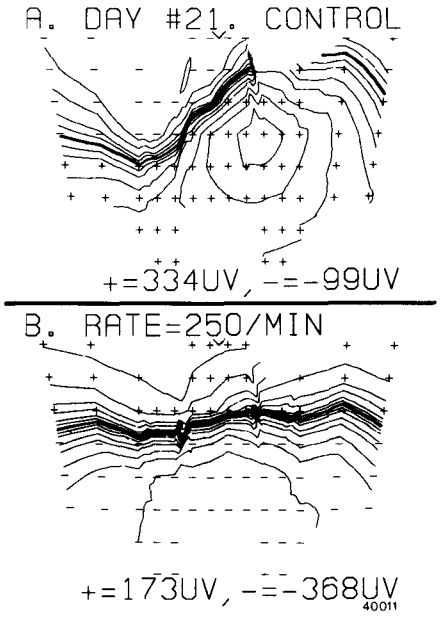

Discussion

This study was designed to explore the electrocardiographic effects of tachycardia-induced myocardial ischemia. An ameroid constrictor generated progressive coronary stenosis, atrial pacing produced transient ischemia and body surface isopotential mapping techniques detected the resulting electrocardiographic changes.

Advantages of the Experimental Methods

Each of these methods was selected on the basis of previously reported advantages. First, the ameroid constrictor, composed of a hygroscopic casein derivative, produces progressive luminal obliteration by absorption of water, fibroblastic response and, occasionally, by intravascular thrombosis (10–12). The coronary hemodynamic consequences of this form of occlusion have been repeatedly studied. Complete vascular occlusion occurs approximately 17 to 25 days (13–15) after surgical implantation. This has been documented by flow measurements reported by Kumada et al. (21); by 23 days after implantation of an ameroid device, half of experimental animals had no flow through the affected coronary artery and the remaining half had reduced flow corresponding to an 85 to 90% luminal narrowing. Similarly, velocity measurements reported by Tomoike et al. (22) demonstrated normal values at rest during the first week after implantation, moderate reduction after 15 to 18 days and marked reductions after 20 to 24 days. Significant collateral vessel development does occur with time, but remains limited during the occlusive phase (13,15,16). Thus, as used in this study, the ameroid device was expected to produce a near total occlusion of the circumflex artery over

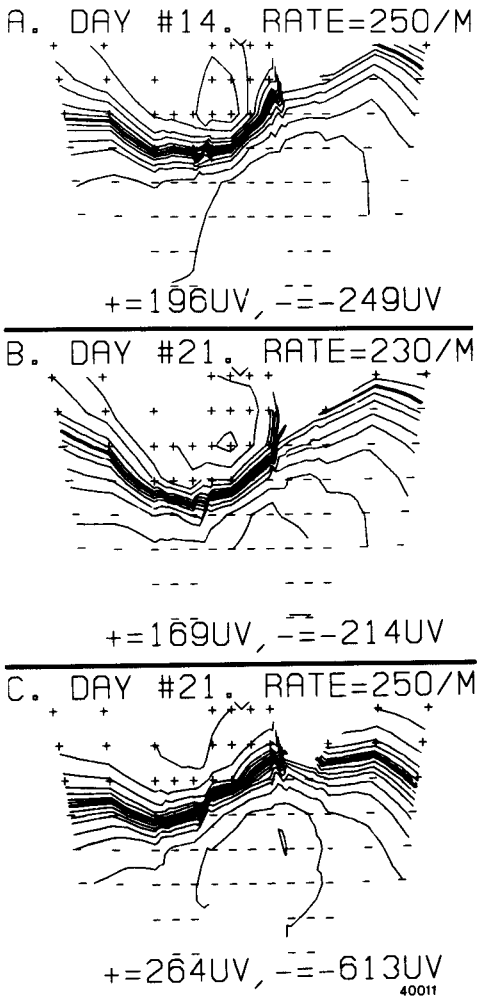

Figure 8. Isopotential difference maps computed as in Figure 3C. **Panel A**, 2 weeks postoperatively (pacing rate 250 beats/min). **Panel B**, 3 weeks postoperatively (rate 230 beats/min). **Panel C**, 3 weeks postoperatively (rate 250 beats/min).

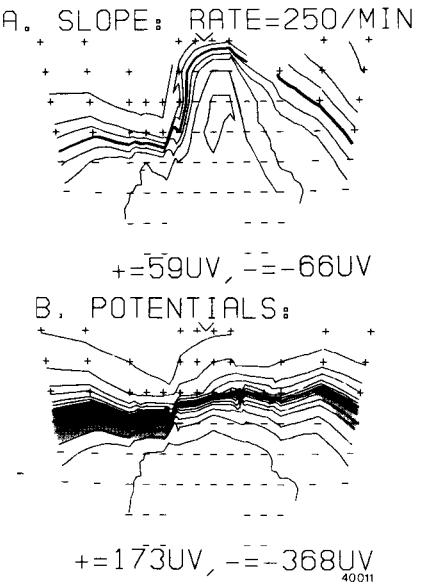

Figure 9. Panel A, Isoslope map, constructed as in Figure 3, depicting the distribution of slopes of the early (10 to 40 ms) ST segment at a paced rate of 250 beats/min 3 weeks after ameroid implantation. **Panel B**, Isopotential distrbution 3 weeks after ameroid placement, 40 ms into ST segment at a paced rate of 250 beats/min. The **shaded areas** represent zones with negative potentials but with positive ST segment slopes, that is, upsloping ST segment depression.

the 3 week period of study with minimal to moderate collateral development.

Second, atrial pacing produces increased myocardial oxygen demand by increasing both rate and inotropic state (23). In dogs without coronary obstruction, this demand and possibly other factors as well (1) resulted in increased total coronary blood flow. For example, Neill et al. (2) and Cobb et al. (1) reported 50% increases in flow with doubling of heart rates. This response stabilized after approximately 30 seconds of an increased rate and peaked at a ventricular rate of 240 beats/min (1). Although some redistribution of blood flow through the ventricular wall occurs (1–3,6), no subendocardial ischemia results with rates under 270 beats/min (2,3,6). Thus, the atrial pacing protocol used here would increase coronary flow in normal dogs almost to the expected maximum without causing ischemia.

In the presence of coronary stenosis, tachycardia causes relative subendocardial underperfusion (4,5,7–9). This has been documented using acute ligation (8), subtotal occluder devices (4,5,9) or ameroid constrictors (7) to limit coronary flow, and exercise (5,7,8) or pacing (4,7,9) to produce tachycardia. For example, Neill et al. (4), reported a reduction in endocardial/epicardial flow ratio from 1.31 during control states to 1.15 with stenosis sufficient to reduce circumflex coronary flow by 20% and to 0.67 with superimposed atropine-induced tachycardia. The degree of subendocardial ischemia increases as the degree of obstruction increases (5), but is unaffected by the mode of tachycardia induction such as exercise or pacing (7). Thus, atrial pacing after ameroid constrictor implantation would produce a degree of subendocardial ischemia similar to that reported during exercise, in direct proportion to the elapsed time after surgery and hence to the degree of vascular occlusion. Exercise protocols could not have been performed because of the excessive electrical noise generated by motor-driven devices. The use of serial, graded increments in rate was designed to reproduce the procedures used in clinical exercise testing.

There is a common but not universal agreement that subendocardial underperfusion and ischemia should result in body surface ST segment depression. Subendocardial mechanical or chemical damage has been shown to produce subendocardial and cavitary ST segment elevation and epicardial and/or precordial ST segment depression (24,25).

Guyton et al. (26) more recently demonstrated that isolated subendocardial underperfusion produced by partial coronary artery obstruction and tachycardia, that is, the model used in this report, also produced epicardial ST segment depression. However, Prinzmetal et al. (27) alternatively suggested that mild subepicardial ischemia may generate ST depression independent of subendocardial damage. Kjekshus et al. (28) reported poor correlation between subendocardial perfusion and ST segment depression. Thus, it does seem that subendocardial damage can cause ST depression on the body surface, although other mechanisms may be operative in certain conditions.

The advantages of surface isopotential mapping, the third technique utilized, over other electrocardiographic techniques have been explored (19). These include the wide torso zones sampled and the ability to evaluate spatial and intensity factors that determine local potentials. The net result was a model intended to simulate the clinical exercise stress test. Advantages of a canine model include 1) control of the number and site(s) of arterial lesions, 2) control of heart rate, 3) ability to study progressive grades of coronary occlusion with considerable time compression, and 4) potential use in study of drug and other interventions that would not be possible in patients.

Limitations of this method. There are, however, certain methodologic limitations of this technique. These include technical concerns, such as superposition of P waves on T waves and ST segments that precluded study of late repolarization phases. In addition, it was necessary to record data relatively early after the surgical procedure when volume conductor properties may not be normal; however, recent data from this laboratory suggested that changes in torso conductivity induced by operation are largely resolved within 2 weeks (29). Because of the progressive evolution of the coronary lesion with time, it was not possible to determine the reproducibility of a pattern in any given dog. Differences between torso geometries and native and collateral coronary physiologic states in the dog and in human beings certainly restrict quick and automatic extrapolation of current findings to the clinical environment; however, data demonstrating only small degrees of collateral flow early after ameroid placement, and the epicardial location of such vessels (whereas ischemia is in subendocardial layers) (15), support the relevance of this model.

Clinical Implications

These limitations notwithstanding, four features described in the report are significant. First, tachycardia in the absence of coronary constriction produced increased electrocardiographic potentials during the early ST segment without changes in the spatial distribution of these voltages (Fig. 2). These differences are less than those reported in human subjects during exercise from this laboratory (30) using TP segment baseline or by Miller et al. (31), using a PR segment reference level. Whether these variations are due to alternate mechanisms of inducing tachycardia, species differences or other causes is unknown.

Second, the electrocardiographic abnormalities typical of myocardial ischemia induced by exercise in human beings, that is, horizontal or downsloping ST segment depression, were consistently generated (Fig. 4, 6 and 7). These evolved consistent with the kinetics of ameroid constriction, in that ischemia first appeared 2 weeks after placement when luminal diameter would be reduced by approximately 60% (15). The ischemic abnormalities became more intense with increased severe narrowing (Fig. 7). Such changes were not seen at equivalent rates in the absence of coronary narrowing or with lesser reductions in luminal size, as during the first week after ameroid implantation. These findings, consistent with known principles of coronary flow in normal and pathologic states (1–9), demonstrate that the model behaved in a manner directly analogous to clinical exercise testing.

Third, ischemia induced a reproducible pattern of precordial ST segment depression. The inferior torso location, most clearly seen in the difference maps of Figure 8, is likely to correspond to the inferoposterior location of myocardium supplied by the left circumflex coronary artery (32). Such a spatial myocardial-torso correlation is consonant with the documented ability of surface isopotential mapping to detect single epimyocardial electrical effects (33). Whether some of the observed ST segment changes may be secondary to the QRS changes known to occur with tachycardia (31) cannot be determined from present data.

Last, and most specifically, the current data provide insight into the variable shape of ST segment depression observed during exercise. Thus, horizontal or downsloping depression is considered highly diagnostic of ischemia; in contrast, upsloping depression has been considered normal or abnormal (34,35). Isopotential and isoslope maps, such as those presented in Figures 3 and 9, demonstrate that downsloping, horizontal and upsloping ST segments may coexist in both normal and ischemia states. This has also been reported in clinical series (34). With ischemia, downsloping ST segments were recorded from sites with maximal segmental depression, whereas upsloping ones were demonstrable from zones with less intense abnormal potentials. If only the latter were sensed, as is reasonable with limited precordial electrode deployment and with certain precordial abnormal distributions, only the upsloping form may be registered. Thus, this diagnostic dilemma may result from an electrocardiographic form of sampling error. The significant percent of torso areas with discordant ST segment voltages and slopes further suggests that these two variables

should be evaluated independently rather than linked as possible diagnostic criteria.

References

1. Cobb FR, Bache RJ, Ebert PA, Rembert JC, Greenfield JC. Effects of beta-receptor blockade on the systemic and coronary hemodynamic response to an increasing ventricular rate in the unanesthetized dog. Circ Res 1969;25:331–41.
2. Neill WA, Phelps NC, Oxendine JM, Mahler DJ, Sim DN. Effect of heart rate on coronary blood flow distribution in dogs. Am J Cardiol 1972;32:306–12.
3. Buckberg GD, Fixler DE, Archie JP, Hoffman JIE. Experimental subendocardial ischemia in dogs with normal coronary arteries. Circ Res 1972;30:67–81.
4. Neill WA, Oxendine J, Phelps N, Anderson RP. Subendocardial ischemia provoked by tachycardia in conscious dogs with coronary stenosis. Am J Cardiol 1975;35:30–6.
5. Ball RM, Bache RJ. Distribution of myocardial blood flow in the exercising dog with restricted artery inflow. Circ Res 1976;38:60–6.
6. Bache RJ, Cobb FR. Effect of maximal coronary vasodilatation on transmural myocardial perfusion during tachycardia in the awake dog. Circ Res 1977;41:648–53.
7. Fedor JM, Rembert JC, McIntosh DM, Greenfield JC. Effects of exercise- and pacing-induced tachycardia on collateral flow in the awake dog. Circ Res 1980;46:214–20.
8. Hess DS, Bache RJ. Regional myocardial blood flow during graded treadmill exercise following circumflex coronary artery occlusion in the dog. Circ Res 1980;47:59–68.
9. Gerry JL, Schaff HV, Kallman CH, Flaherty JT. Effects of nitroglycerin on regional myocardial ischemia induced by atrial pacing in dogs. Circ Res 1981;48:569–76.
10. Berman JK, Fields DC, Judy H, Mari V, Parker RJ. Gradual vascular occlusion. Surgery 1956;39:399–410.
11. Litvak J, Siderides LE, Vineberg AM. The experimental production of coronary artery insufficiency and occlusion. Am Heart 1957;53:505–18.
12 Vineberg A, Mahanti B, Litvak J. Experimental gradual coronary artery constriction by ameriod constrictors. Surgery 1960;47:765–71.
13. Elliott EC, Jones EL, Bloor CM, Leon AS, Gregg DE. Day-to-day changes in coronary hemodynamics secondary to constriction of the circumflex branch of left coronary artery in conscious dogs. Circ Res 1968;22:237–50.
14. Flameng W, Schaper W, Lewi P. Multiple experimental coronary occlusion without infarction. Am Heart J 1973;85:767–76.
15. Scheel KW, Granger HJ, Brody DA, Keller FW. Mechanisms of collateral development and hemodynamics of gradual coronary occlusion. Basic Res Cardiol 1974;69:338–60.
16. Scheel KW, Galendez TA, Cook B, Rodriquez RJ, Ingram LA. Changes in coronary and collateral flow and adequacy of perfusion in the dog following one and three months of circumflex occlusion. Circ Res 1976;39:654–8.
17. Cox JW, Laughter JS, Brandon CW, et al. A systems oriented ECG amplifier. Cardiovasc Res 1979;13:238–41.
18. Brody DA, Woolsey MD, Arzbaecher RC. Application of computer techniques to the detection and analysis of spontaneous P-wave variations. Circulation 1967;36:359–68.
19. Spach MS, Barr RC, Warren RB, Benson DW, Walston A, Edwards SB. Isopotential body surface mapping in subjects of all ages: emphasis on low-level potentials with analysis of the method. Circulation 1979;59:802–21.
20. Eddlemon CO, Ruesta VJ, Horan LG, Brody DA. Distribution of heart potentials on the body surface of five normal young men. Am J Cardiol 1968;21:860–9.
21. Kumada T, Gallagher KP, Shirato K, et al. Reduction of exercise-induced regional myocardial dysfunction by propranolol. Circ Res 1980;46:190–200.
22. Tomoike H, Franklin D, Kemper WS, McKown D, Ross J. Functional evaluation of coronary collateral development in conscious dogs. Am J Physiol 1981;241:H519–24.
23. Boerth RC, Covell JW, Pool PE, Ross J. Increase myocardial oxygen consumption and contractile state associated with increased heart rate in dogs. Circ Res 1969;24:725–34.
24. Wolferth CC, Bellet S, Livezey MM, Murphy FO. Negative displacement of the RS-T segment in the electrocardiogram and its relationships to positive displacement. Am Heart J 1945;29:220–45.
25. Zakopoulos KS, Herrlich HC, Lepeschkin E Effect of subendocardial injury on the electrocardiogram of intact dogs. Am J Physiol 1967;213:143–7.
26. Guyton RA, McClenathan JH, Newman GE, Michaelis LL. Significance of subendocardial S-T segment elevation caused by coronary stenosis in the dog. Am J Cardiol 1977;40:373–80.
27. Prinzmetal M, Toyoshima H, Ekmekci A, Mizuno Y, Nagaya T. Myocardial ischemia. Nature of ischemic electrocardiographic patterns in the mammalian ventricles as determined by intracellular electrographic and metabolic changes. Am J Cardiol 1961;8:493–503
28. Kjekshus JK, Maroko PR, Sobel BE Distribution of myocardial injury and its relation to epicardial ST segment changes after coronary artery occlusion in the dog. Cardiovasc Res 1972;6:490–9
29. Mirvis DM. Effects of thoracotomy on volume conductor properties of the canine torso. J Electrocardiol (in press).
30. Mirvis DM, Keller FW, Cox JW, Zettergren DG, Dowdie RF, Ideker RE. Left precordial isopotential mapping during supine exercise. Circulation 1977;56:245–53.
31. Miller WT, Spach MS, Warren RB. Total body surface potential mapping during exercise: QRS-T-wave changes in normal young adults. Circulation 1980;62:632–45.
32. Scheel KW, Ingram LA, Gordey RL. The relationship of coronary flow and perfusion territory in the dog. Am J Physiol 1982;243:H738–47.
33. Abildskov JA, Burgess MJ, Lux RL, Wyatt RF. Experimental evidence for regional cardiac influence in body surface isopotential maps of dogs. Circ Res 1976;38:386–91.
34. Chaitman BR, Bourassa MG, Wangiart P, Corbara F, Ferguson RJ. Improved efficiency of treadmill exercise testing using a multiple lead ECG system and basic hemodynamic exercise response. Circulation 1978;57:71–9.
35. Goldschlager N, Selzer A, Cohn K. Treadmill stress tests as indicators of presence and severity of coronary artery disease. Ann Intern Med 1976;85:277–86.